

# Topology and Analysis of An Electromechanical Brake for Electric Vehicles

Xiangdang XUE, Ka Wai Eric CHENG, and Yulong FAN

Power Electronics Research Centre, Department of Electrical Engineering, The Hong Kong Polytechnic University, Hong Kong, China  
E-mail: xd.xue@polyu.edu.hk, eecheng@polyu.edu.hk

**Abstract**– A new automotive electromechanical brake (EMB) is proposed in this study, which consists of the electromagnetic linear actuator that includes the stator and the mover, the power rod, the wedge, the braking pads, the caliper and the mechanical accessory. The braking torque is controlled via the actuator control unit. The topology structure of the proposed EMB is discussed. The models of the proposed EMB are developed, it is confirmed that the proposed EMB provides two braking forces with same magnitude and opposite direction to the braking pads, and the gains of the components and the proposed EMB are formulated. Furthermore, the effects of the geometrical parameter and the design parameter on the performance of the proposed EMB are analyzed via simulation. This study provides a novel EMB topology for electric vehicles, which possesses the faster dynamic response than previous EMBs.

**Keywords**–Braking system, electric vehicles (EV), electromechanical brake (EMB).

## I. INTRODUCTION

For current commercial automobiles, hydraulic or electrohydraulic wheel brakes are used popularly. However, those brakes possess the inherent disadvantages, such as the flammable braking fluid, the leakage of the braking fluid and the discontinuous control of the braking torque, which degraded automotive safety, ABS performance and environmental protection. An alternative solution is being concerned, which is the electromechanical brake (EMB) [1]-[5]. Without any hydraulic component, the electromechanical brakes are controlled electrically. The electromechanical brakes have a number of potential advantages compared with conventional electrohydraulic brakes, such as faster dynamic response, more accurate braking torque control, continuous control of braking torque, improved braking and stability behavior, no flammable fluids, and reduction in complexity and quantity of components. Thus, the electromechanical brakes are regarded as the next generation of automotive wheel brakes.

## II. TOPOLOGY OF PROPOSED ELECTROMECHANICAL BRAKE

Fig. 1 illustrates the topology of the proposed electromechanical brake. It consists of the electromagnetic linear actuator that includes the stator and the mover, the power rod, the wedge, the braking pads, the caliper and the accessory.

The operation of the proposed electromechanical brake can be summarized as follows. The electromagnetic linear actuator is controlled by its control unit, in which the input voltage signal is used to control the electromagnetic force

output by the mover. The electromagnetic force is appropriately proportional to the input voltage signal. Via the mechanical link between the mover and the right terminal of the power rod, the electromagnetic force is transferred to the right terminal of the power rod. Due to the mechanism of the power pod, the force applied to the right terminal of the power rod is transferred to the left terminal of the power pod. Via the mechanical link between the left terminal of the power rod and the wedge, the force applied to the left terminal of the power rod is transferred to the wedge. Consequently, the force applied to the wedge makes the wedge move up or down. The up motion of the wedge further results in that the right braking pad moves left, and the caliper moves right. Moreover, the right motion of the caliper makes the left braking pad moves right. Thereby, two braking pads move toward the braking disc, until two braking pads contact the braking disc to generate the braking torque applied to the braking disc. The electromagnetic force is zero and the wedge and two braking pads release if the input voltage signal is zero.

The effect diagram that the proposed electromechanical brake is applied to the automotive wheel is shown in Fig. 2.

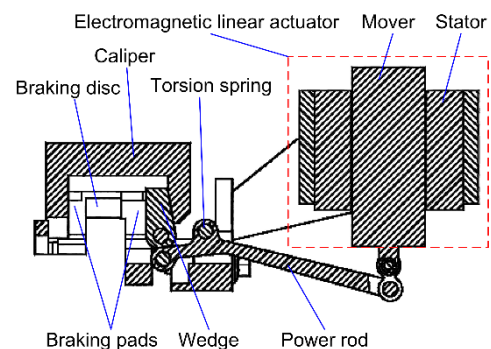


Fig. 1 Topology of proposed electromechanical brake

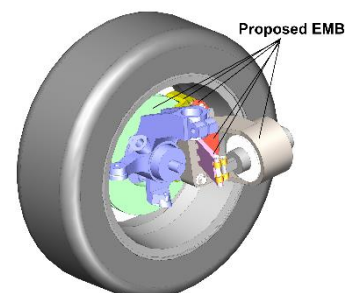


Fig. 2 Integration between wheel and proposed electromechanical brake

The electromechanical brake unit consists of the electromechanical brake and the actuator control unit. The schematic structure of the electromechanical brake unit is illustrated in Fig. 3.

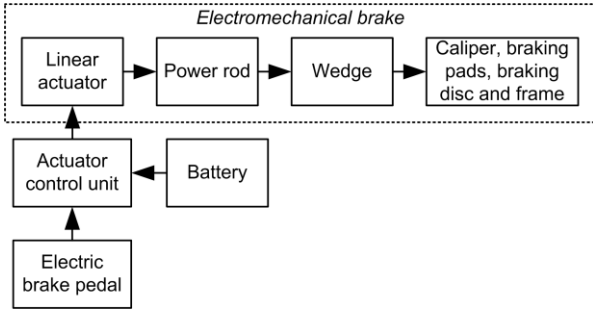


Fig. 3 Control schematic of proposed electromechanical brake

### III. MODELS OF PROPOSED ELECTROMECHANICAL BRAKE

#### 1. Model of Electromagnetic Linear Actuator

The model of the electromagnetic linear actuator is illustrated in Fig. 4, in which the input voltage signal ( $V_{in}$ ) is converted into the electromagnetic force ( $F_{em}$ ) by the electromagnetic linear actuator and the conversion coefficient is  $K_c$ . It is assumed that the electromagnetic linear actuator generates the down electromagnetic force in the subsequent analysis, in which the gravities of all the components are neglected.

Referring to Fig. 4, the relationship between the electromagnetic force output by the mover and the voltage signal input to the control unit of the electromagnetic linear actuator can be expressed as

$$F_{em} = K_c V_{in} \quad (1)$$

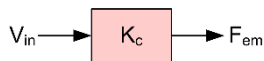


Fig. 4 Model of electromagnetic linear actuator

#### 2. Model of Power Rod

Fig. 5 illustrates the model of the power rod, in which  $F_{rt}$  represents the force applied to the right terminal of the power rod,  $L_r$  the length of the right arm of the power rod,  $F_{lt}$  the force applied to the left terminal of the power rod, and  $L_l$  the length of the left arm of the power rod.

The force ( $F_{rt}$ ) applied to the right terminal of the power rod is equal to the electromagnetic force ( $F_{em}$ ) if the loss of

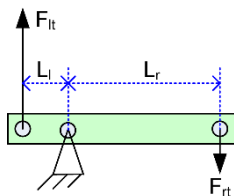


Fig. 5 Model of power rod  
International Conference on Power Electronics Systems and Applications (PESA 2020)

the mechanical link is ignored. Thus, one has

$$F_{rt} = F_{em} \quad (2)$$

At the same time, the force applied to the left terminal of the power rod can be calculated as

$$F_{lt} = \frac{L_r}{L_l} F_{rt} \quad (3)$$

#### 3. Model of Wedge

The model of the wedge is illustrated in Fig. 6 when the wedge and the caliper are at standstill. In Fig. 6,  $\alpha$  represents the wedge angle,  $F_{rw}$  the force applied to the wedge by the left terminal of the power rod,  $F_{pw}$  the normal force applied to the wedge by the right braking pad,  $F_{cw}$  the normal force applied to the wedge by the caliper,  $F_{fpw}$  the friction force between the right braking pad and the left wedge surface, and  $F_{fcw}$  the friction force between the caliper slope surface and the wedge slope surface.

The force balance equation in the horizontal direction can

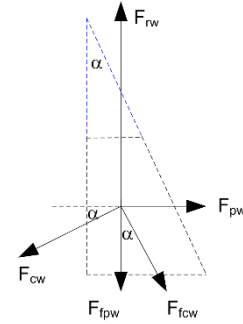


Fig. 6 Model of wedge

be expressed as

$$F_{cw} \cos \alpha = F_{pw} + F_{fcw} \sin \alpha \quad (4)$$

The force balance equation in the vertical direction can be given as

$$F_{rw} = F_{cw} \sin \alpha + F_{fpw} + F_{fcw} \cos \alpha \quad (5)$$

where  $F_{rw}$  is equal to  $F_{lt}$ .

The friction force between the right braking pad and the wedge can be calculated as

$$F_{fpw} = \mu_f F_{pw} \quad (6)$$

where  $\mu_f$  is the friction coefficient.

The friction force between the caliper and the wedge can be calculated as

$$F_{fcw} = \mu_f F_{cw} \quad (7)$$

#### 4. Model of Caliper

The model of the caliper is shown in Fig. 7 when the wedge and the caliper are at standstill. In Fig. 7,  $F_{wc}$  represents the normal force applied to the caliper by the wedge,  $F_{pc}$  the normal force applied to the caliper by the left braking pad,  $F_{fwc}$  the friction force between the wedge slope surface and the caliper slope surface, and  $F_{sc}$  the force applied to the caliper by the support.

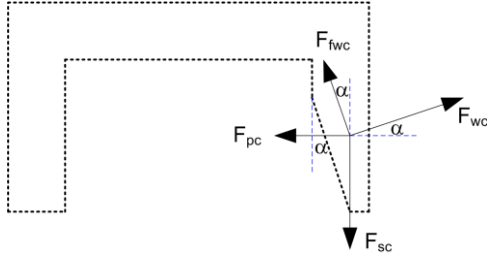


Fig. 7 Model of caliper

The force balance equation in the horizontal direction can be expressed as

$$F_{wc} \cos \alpha = F_{pc} + F_{f_{wc}} \sin \alpha \quad (8)$$

The force balance equation in the vertical direction can be given as

$$F_{sc} = F_{wc} \sin \alpha + F_{f_{wc}} \cos \alpha \quad (9)$$

Furthermore, one has

$$F_{f_{wc}} = F_{f_{cw}} \quad (10)$$

$$F_{wc} = F_{cw} \quad (11)$$

$$F_{wp} = F_{pw} \quad (12)$$

$$F_{cp} = F_{pc} \quad (13)$$

where  $F_{cp}$  represents the normal force applied to the left braking pad by the caliper.

#### 5. Braking Force Applied to Two Braking Pads

From the equations (4) (7), the normal force applied to the wedge by the right braking pad can be calculated as

$$F_{pw} = F_{cw} - \mu_f F_{cw} \sin \alpha \quad (14)$$

From the equations (8) (10) (11), the normal force applied to caliper by the left braking pad can be expressed as

$$F_{pc} = F_{cw} - \mu_f F_{cw} \sin \alpha \quad (15)$$

Referring to the equations (12)-(15), it can be seen that the normal force applied to the right braking pad is equal to the normal force applied to the left braking pad. In other words, thus, the braking force applied to the right braking pad and the braking force applied to the left braking pad have the same magnitude and the opposite direction. It meets the requirement of the wheel brakes.

#### 6. Vertical Displacement of Wedge and Horizontal Displacement of Braking Pads

The wedge only moves vertically in the proposed electromechanical brake. Due to the wedge's structure, however, the wedge is capable of generating the horizontal displacement if the wedge moves vertically to result in the vertical displacement. The relationship between the vertical wedge displacement and the horizontal wedge displacement is shown in Fig. 8, if the wedge moves upward.

If the vertical wedge displacement is  $D_y$ , referring to Fig. 8, the horizontal wedge displacement ( $D_x$ ) can be calculated as

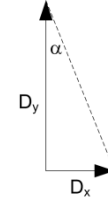


Fig. 8 Vertical and horizontal displacements of wedge

$$D_x = D_y \tan \alpha \quad (16)$$

The horizontal displacement generated by the wedge results in that two braking pads move toward the braking disc. Consequently, the relationship between the horizontal wedge displacement and the horizontal displacement of the braking pad ( $D_p$ ) can be expressed as

$$D_x = 2D_p \quad (17)$$

Thereby, the relationship between the vertical wedge displacement and the horizontal displacement of the braking pad can be expressed as

$$D_y = \frac{2D_p}{\tan \alpha} \quad (18)$$

#### 7. Gains of Proposed Electromechanical Brake

Table I shows the gains of three components and the proposed electromechanical brake. The gain of the electromagnetic linear actuator ( $G_a$ ) is defined as the ratio of the electromagnetic force to the input voltage signal, the gain of the power rod ( $G_r$ ) is defined as the ratio of the force applied to the left rod terminal to the force applied to the right rod terminal, the gain of the wedge ( $G_w$ ) is defined as the ratio of the force applied to the right braking pad by the wedge and the force applied to the wedge by the left rod terminal, and the gain of the electromechanical brake ( $G_{EMB}$ ) is defined as the ratio of the force applied to the right braking pad by the wedge to the input voltage signal. These gains can be obtained from the equations (1)-(15).

Table 1: Gains of proposed electromechanical brake

Gain	Value
$G_a$	$K_c$
$G_r$	$L_r/L_l$
$G_w$	$\frac{\cos \alpha - \mu_f \sin \alpha}{\sin \alpha + 2\mu_f \cos \alpha - \mu_f^2 \sin \alpha}$
$G_{EMB}$	$\frac{K_c L_r (\cos \alpha - \mu_f \sin \alpha)}{L_l (\sin \alpha + 2\mu_f \cos \alpha - \mu_f^2 \sin \alpha)}$

#### IV. ANALYSIS OF PROPOSED ELECTROMAGNETIC BRAKE

##### 1. Effect of Wedge Angle on Gain of Wedge

For the proposed electromechanical brake, it can be seen from Table I that the gain of the wedge depends on the

wedge angle and the friction coefficient. The effect of the wedge angle on the wedge's gain is illustrated in Fig. 9 if the friction coefficient is equal to 0.1. It can be observed from Fig. 9 that the gain of the wedge decreases for the specified friction coefficient if the wedge angle becomes large. Consequently, the wedge angle should be designed as the small angle, to obtain the high gain of the wedge.

### 2. Effect of Friction Coefficient on Gain of Wedge

Fig. 10 illustrates the effect of the friction coefficient on the wedge's gain if the wedge angle is 15 degree. It can be observed from Fig. 10 that the gain of the wedge decreases for the specified wedge angle if the friction coefficient between the wedge surfaces and the other surfaces becomes high. Thereby, the friction coefficient should be selected as the low value, to obtain the high gain of the wedge.

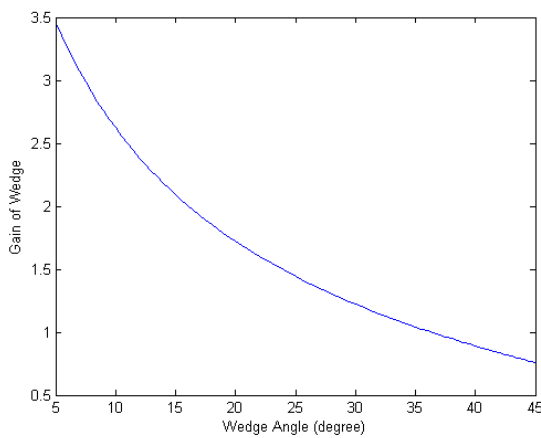


Fig. 9 Effect of wedge angle on wedge's gain

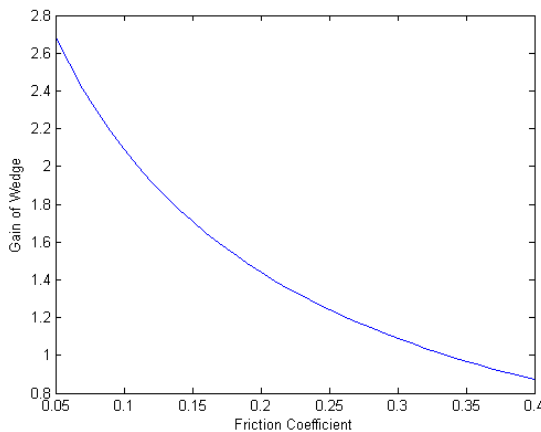


Fig. 10 Effect of friction coefficient on wedge's gain

### 3. Effect of Wedge Angle on Maximum Displacement of Braking Pad

The effect of the wedge angle on the maximum displacement of the braking pad is shown in Fig. 11 if the maximum vertical displacement of the wedge is 10 mm. It can be seen from Fig. 11 that the maximum displacement

of the braking pad increases for the specified maximum vertical displacement of the wedge if the wedge angle becomes large. Therefore, the wedge angle should be designed appropriately, to guarantee that the maximum displacement of the braking pad is more than the clearance of the braking pad, which is the distance between the braking disc and the braking pad at the releasing position of the braking pads.

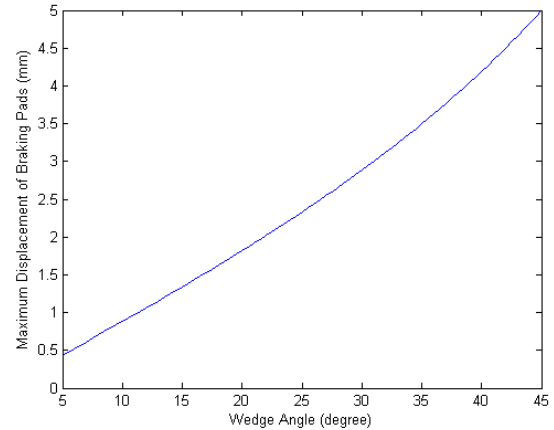


Fig. 11 Effect of wedge angle on maximum displacement of braking pads

## V. CONCLUSION

The electromechanical brake with the new topology and behavior has been proposed in this paper, which is applicable to wheel brakes in electric vehicles and controlled electrically without any hydraulic component. The models of the components in the proposed electromechanical brake have been developed, which can be used to complete the design of the proposed electromechanical brake. The theoretical analysis has confirmed that the braking force applied to the right braking pad and the braking force applied to the left braking pad have the same magnitude and the opposite direction. The simulation analysis shows that the wedge angle has the considerable effects on the gain of the wedge and the maximum displacement of the braking pads for the specified maximum vertical displacement of the wedge, and the friction coefficient between the wedge surfaces and the surfaces of other components has the significant effect on the gain of the wedge. The wedge angle should be selected appropriately, to obtain the sufficiently high gain of the wedge and the enough large displacement of the braking pads. The friction coefficient should be designed as low as possible, to obtain the high gain of the wedge.

## ACKNOWLEDGMENT

The authors would like to thank the part financial support from the Guangdong-Hong Kong Technology Cooperation Funding Scheme of Hong Kong Innovation and Technology Support Programme under Grant GHP/033/17AP.

## REFERENCES

- [1] Reza Hoseinnezhad, Alireza Bab-Hadiashar, and Tony Rocco, "Real-Time Clamp Force Measurement in Electromechanical Brake Calipers", IEEE TRANSACTIONS ON VEHICULAR TECHNOLOGY, VOL. 57, NO. 2, MARCH 2008, pp. 770-777, DOI 10.1109/TVT.2007.906374.
- [2] Chihoon Jo, Sungho Hwang, and Hyunsoo Kim, "Clamping-Force Control for Electromechanical Brake", IEEE TRANSACTIONS ON VEHICULAR TECHNOLOGY, VOL. 59, NO. 7, SEPTEMBER 2010, pp. 3205-3212 DOI 10.1109/TVT.2010.2043696.
- [3] Jiweon Ko, Sungyeon Ko, Hanho Son, Byoungsoo Yoo, Jaeseung Cheon, and Hyunsoo Kim, "Development of Brake System and Regenerative Braking Cooperative Control Algorithm for Automatic-Transmission-Based Hybrid Electric Vehicles", IEEE TRANSACTIONS ON VEHICULAR TECHNOLOGY, VOL. 64, NO. 2, FEBRUARY 2015, pp. 431-440, DOI 10.1109/TVT.2014.2325056.
- [4] Heeram Park and Seibum B. Choi, "Development of a Sensorless Control Method for a Self-Energizing Brake System Using Noncircular Gears", IEEE TRANSACTIONS ON CONTROL SYSTEMS TECHNOLOGY, VOL. 21, NO. 4, JULY 2013, pp. 1328-1339, DOI 10.1109/TCST.2012.2204750.
- [5] Sangjune Eum, Jihun Choi, Sang-Shin Park, Changhee Yoo and Kanghyun Nam, "Robust Clamping Force Control of an Electro-Mechanical Brake System for Application to Commercial City Buses", Energies 2017, 10, 220, pp. 1-12, DOI 10.3390/en10020220.